https://doi.org/10.17221/122/2021-JFS

Burned area determination using Sentinel-2 satellite images and the impact of fire on the availability of soil nutrients in Syria

Rukea Al-hasn, Raed Almuhammad*

General Commission for Scientific Agricultural Research (GCSAR), Damascus, Syria

**Corresponding author: rukeaalhasn@gmail.com*

Citation: Al-hasn R., Almuhammad R. (2022): Burned area determination using Sentinel-2 satellite images and the impact of fire on the availability of soil nutrients in Syria. J. For. Sci., 68: 96–106.

Abstract: The objective of this research is the identification of burned forest areas that occurred in Syria from September 2nd to October 15th, 2020. Forest fire risk classes were determined using Sentinel-2 images. Normalized Burn Ratio (*NBR*), Differenced Normalized Burn Ratio (*dNBR*), and Burned Area Index for Sentinel-2 (*BAIS*2), and Normalized Difference Vegetation Index (*NDVI*) were used for the identification how much the forests have been destroyed and to establish fire risk classes. According to the study results, the size of the vegetation area that was destroyed due to fire was determined, and the probability of the forest fire exposure of these areas was established. The fires also altered some chemical properties in the soil during the combustion process. Thus, this study was focused on the impact of fire on the availability of soil nutrients. Soil samples were collected from three depths (0–10 cm, 10–20 cm and 20–30 cm) under the forest land a month after the fire in three locations: Al-Fazeen, Sawda and Gard Al-rihan. Pine (*Pinus brutia*) trees cover these areas. The results of this study indicated that the fire increased pH, EC and sand, the fire also led to an increase in the solubility of the available major soil elements N, P and K. There was an increase in the solubility of the soil microelements Zn, Cu, Mn and Fe while the content of organic material and silt and clay ratio decreased at the three sites in comparison with unburned soil.

Keywords: burned forest; *NBR*; *dNBR*; *BAIS*2; *NDVI*

From the past to the present, a global pattern of increasing forest fires has been recorded. The literature defines the fire intensity in a fire environment as an impact of the fire on the ecosystem (Sugihara et al. 2006). The natural environment is disrupted as a result of these fires which cause harm to enormous natural areas, as well as human and living creature deaths. There are two main factors that cause forest fires: nature and humans. Forest fires are caused by a number of circumstances, including unplanned urbanization, sabotage, carelessness, irresponsibility, and global warming. Many large forest fires have erupted around the world in recent years; 271 350 ha of land in Greece in 2007, 450 000 ha in Australia in 2009, and 500 000 ha in Russia in 2010 were destroyed. In addition, 25 000 ha in Bolivia in 2010 were ravaged by fires. The forest fire in Canada destroyed 1 200 000 ha of land in 1825, and this was recorded as the largest known forest fire in history (Francos et al. 2016). Forest fires have been reported in France, Greece, Italy, Portugal and Spain, more than 450 000 ha were burned annually between 2000 and 2006, and in 2007 the burned area amounted to about 500 000 ha.

https://doi.org/10.17221/122/2021-JFS

Most of them occur in Italy and Greece (Bassi, Kettunen 2008) while most of the Mediterranean Basin fires are a consequence of anthropogenic activities and are not normal (Espelta et al. 2008). However, the frequency of fires is expected to increase due to global warming, changes in the rainfall regime and the length of the rainy season (Pausas 2004). The Mediterranean countries are among the most affected by fires (Quintano et al. 2018). Fires are among the main reasons for environmental alteration in the ecosystems of the forest. In the Mediterranean, forest cover and fire recovery are monitored for fire management and plan. It is important that the burned areas and the intensity of the fires are known accurately (Brewer et al. 2005; Fernández-Manso, Quintano 2015).

In the Mediterranean countries, studies have shown an increase in the extent, area, and frequency of combustion (Pausas et al. 2008). Like within all countries in the Mediterranean region, the fires are the main threat to forests in Syria (Ali 2000, 2004). Fires are the most dangerous form of encroachment on Syrian forests due to the sudden change in the environment surrounding these forests. Annually, the fires consume the equivalent of 755.19 ha of our forests, most of which consist of *Pinus brutia* (Kasas 2008). The 2002 damage caused by forest fires is most severe in felled areas (Rowell, Moore 2003). Remote sensing can be used to recognize areas affected by forest fires, as well as to classify these areas according to the likelihood of wildfires. For so long, forest fire damage has been revealed by remote sensing methods (Yurtseven 2014). Remote sensing provides a new window for understanding the reasons, processes, and effects of forest fires, and utilizes geographic techniques (Gupta et al. 2018).

In detecting and monitoring the regions with forest fire danger, remote sensing also offers speed, practicality, and efficiency. The use of remote sensing in the identification of forest fires has become more common as technology advances. Damage detection studies and the detection of risk areas has increased gradually and there are many studies on this subject (Kerr, Ostrovsky 2003; Boer et al. 2008; Matin et al. 2017; Navarro et al. 2017; Yuan et al. 2017). Remote sensing is one of the tools that provide a timely reception of measurements with the growth of technology. Remote sensing could be used to identify areas damaged by forest fires, and besides, these areas could be classified according to forest fire possibility.

The chemical and physical properties of soil can be greatly affected by forest fires, which also affect soil erosion and can affect the entire vegetation cover (SCBD 2001). Fires can also cause a number of organic and inorganic changes in the soil (Ursino, Rulli 2010).

This study aims to detect the area destroyed by fire by means of remote sensing and to evaluate the fire risk in other areas. In this context, Sentinel-2 images were used in order to detect the forest fire risk class. Normalized Burn Ratio (*NBR*), Burned Area Index for Sentinel-2 (*BAIS*2), Differenced Normalized Burn Ratio (*dNBR*), and Normalized Difference Vegetation Index (*NDVI*) were used to determine the forest areas damaged by fire and to identify the fire hazard classes.

MATERIAL AND METHODS

Study area. The research area is situated in the northwestern part of Syria between 34°18'00''N and 36°26'00''N and 35°40'00''E and 37°28'00''E. The portion of the affected territory encompasses Lattakia, Tartous and part of Hama and Idlib provinces (Figure 1). In addition, it has been classified as a high-risk area and rated with a very high probable risk index (Forestry and Reforestations Directorate 2005). The type of climate found in the study area is called semi-moderate oceanic average climate, indicating certain dryness during the summer. This means that a large part of the vegetation is adapted to periods of drought. Under this climatic type, pine trees are the predominant vegetation likely prevalent in most of the region. The wildfire incidents occurred in the period between September 2nd and October 15th, 2020.

Data and preprocessing. Remote sensing data from the Sentinel-2 sensor used within the scope of the study were obtained free of charge from the United States Geological Survey (USGS) website (http://earthexplorer.usgs.gov/) in the UTM projection system as defined in the 37th region. Four Sentinel-2 satellite images were used covering the study area, two before the fire taken on September 27th, 2020, and the other two taken after the fire on October 22nd, 2020 (Table 1). The Sentinel-2A satellite images used were without cloud coverage over the entire scenes.

Remote sensing data were analyzed in order to identify the burn severity classes. Sentinel-2 data have high spatial resolution (10–20 m, depending on bands) and high temporal frequency (5 days),

https://doi.org/10.17221/122/2021-JFS

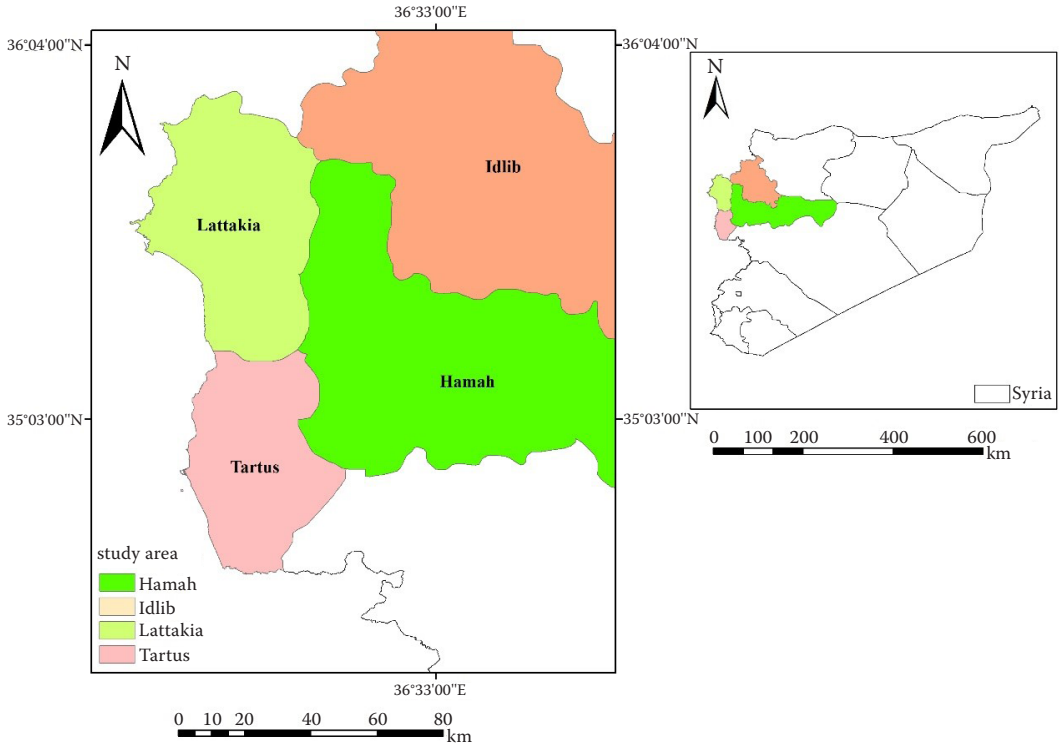

Figure 1. Study area

and recent studies have scrutinized their identification for burned area mapping (Roteta et al. 2019). Topographic factors, atmospheric influences, and shadows must all be eliminated or minimized. Due to effects and sensor-induced errors in satellite images, atmospheric correction is required (Canbaz et al. 2018; Kalkan, Maktav 2018). For this, Sentinel-2 data were atmospherically corrected to L2A bottom of atmosphere reflectance using the Sen2Cor processor algorithm in SNAP program (Main-Knorn et al. 2017), *NBR*, *dNBR*, and *BAIS*2 were performed as spectral indices of forest fire, in addition to *NDVI* index. The indices used were obtained from the electromagnetic spectrum for satellite image Sentinel-2A. These indices were created through images taken before and after fire.

Table 1. The satellite images used in the study, sensor – S2A

Sentinel-2 Scene	Date	Event
L1C_T37SBU_20200927T081719 L1C_T37SBV_20200927T081719	September 27th, 2020	pre-fire
L1C_T37SBU_20201022T082011 L1C_T37SBV_20201022T082011	October 22nd, 2020	post-fire

The Normalized Burn Ratio has been used to watch changes in vegetation caused by fire (Chen et al. 2011; Veraverbeke et al. 2011) in the near-infrared range. Healthy vegetation has a high reflectivity, whereas in the shortwave infrared region, it has a low reflectivity. In addition, the burned areas have low near-infrared reflection but short-wavelength infrared reflection. Therefore, high *NBR* values indicate unburned vegetation, while low values indicate burned areas (Key, Benson 2006). In the next step, the *NBR* difference (*dNBR*) between the pre-fire image and the post-fire image gave an idea of the intensity of the combustion. *BAIS*2 Burned Area Map Spectrum Index has been specifically designed to take advantage of the spectral properties of Sentinel-2 MSI. This index makes use of the characteristics of vegetation described in the red edge spectral domains and the radiative response in the shortwave infrared (SWIR) spectral domain that are largely known to be effective in identifying burned areas (Elvidge 1990). Table 2 shows the forest fire indicators used in the study and their corresponding formulas.

Once the burned area has been mapped using QGIS software (v3.16, 2020), the next stride is the computation of one of the best-known and most

https://doi.org/10.17221/122/2021-JFS

Table 2. Fire indices employed in the study

Fire indices	Formula
NBR	$\frac{B8 - B12}{B8 + B12}$
dNBR	$NBR_{pre\text{-}fire} - NBR_{post\text{-}fire}$
BAIS	$\left(1 - \frac{\sqrt{B6 + B7 + B8A}}{B4}\right) \times \left(\frac{B12 - B8A}{\sqrt{B12 + B8A}} + 1\right)$

NBR – Normalized Burn Ratio; *dNBR* – Differenced Normalized Burn Ratio; *BAIS* – Burned Area Index for Sentinel-2; B4, B6, B7, B8A, B12 – Sentinel-2 spectral bands used for the index calculation

commonly used spectral indices, *NDVI*. It benefits from the feature of green powerful vegetation – absorption of visual red light, as opposed to its high reflection of near-infrared light [Equation (1)].

$$NDVI = \frac{B8 - B4}{B8 + B4} \quad (1)$$

where:
B4, B8 – Sentinel-2 spectral bands used for *NDVI* index calculation.

Determination of thresholds. In this study, we determined the optimal threshold for each spectral index by comparing the burned areas obtained from a reference image (Google Earth image) with those acquired by a sequence of thresholds from a spectral index (Santana et al. 2018).

Validation. The error matrix and its associated precision scale (total precision) which is the ratio of the number of correctly classified samples to the total number of samples (Congalton, Green 2019) were calculated.

Soil samples. The soil was sampled before and after fire from three random locations in the studied area. Soil sampling was done from the depths of 0–10 cm, 10–20 cm, and 20–30 cm under forest land from three sites after burning. Pine (*Pinus brutia*) trees cover these areas. Soil chemical and physical data were estimated in laboratories of the General Commission of Scientific Agricultural Research (GCSAR).

Laboratory analysis. Mechanical analysis was performed on the texture of soil (%), using hydrometer modality (Gee, Or 2002).

Chemical analysis. pH of a saturated paste was extracted using pH meter (Conyers, Davey 1988), EC (electrical conductivity) (Siemens·m^{-1}) in a saturated paste was extracted using EC meter (Rhoades 1996), and percentage of organic matter was determined using the wet oxidization method with dipotassium chromate in a high acidity medium (Nelson, Sommers 1996). Overall nitrogen levels were identified using the Kjeldahl oxidation method (Bremner 1996). Available phosphorous was measured by the Olsen method (Kuo 1996). Available potassium levels were measured with a flame emission spectrometer (Suarez 1996). Diethylenetriaminepentaacetic acid (DTPA) was used to extract micronutrients (iron, manganese, zinc, and copper). Then they were measured using atomic absorption spectrometry (Loeppert, Inskeep 1996). Statistical analyses of the obtained data were processed by two-way analysis of variance (ANOVA) using the R software (4.0.5, 2021), in which soil depth and fire time sequence were chosen as factors (Table 2). The influence of factors (soil depth and fire) and the possible interaction between them was carried out on a 95% probability level (Davies 2016). Fire risk zones and vegetation cover destroyed by fire have been detected using fire indices and *NDVI*.

RESULTS AND DISCUSSION

First, *NBR* and *dNBR* were applied to images. Then, the results of the indices were classified according to pixel values and the regions that pose a fire risk were determined (Figures 2 and 3).

According to the risk severity map made according to the *dNBR* index it is understood that not nearly all of the study area is under a threat of wildfire. Additionally, the sizes of fire severity classes were calculated (Table 3).

The new *BAIS*2 spectral index (Burned Area Index for Sentinel-2) for the mapping of the burned area was used to adopt a spectral set of bands that have been shown to be suitable for the detection of the burned area after a fire. The *dBAIS*2-derived

Table 3. Distribution of calculated areas after applying the Differenced Normalized Burn Ration (*dNBR*)

Fire severity	Area (km^2)	
	September 27th, 2020	October 22nd, 2020
Low to moderate	2 720.30	5 156.48
Moderate to high	3 543.88	3 889.89
High	1 911.30	1 718.41
Sum	8 175.48	10 764.80

https://doi.org/10.17221/122/2021-JFS

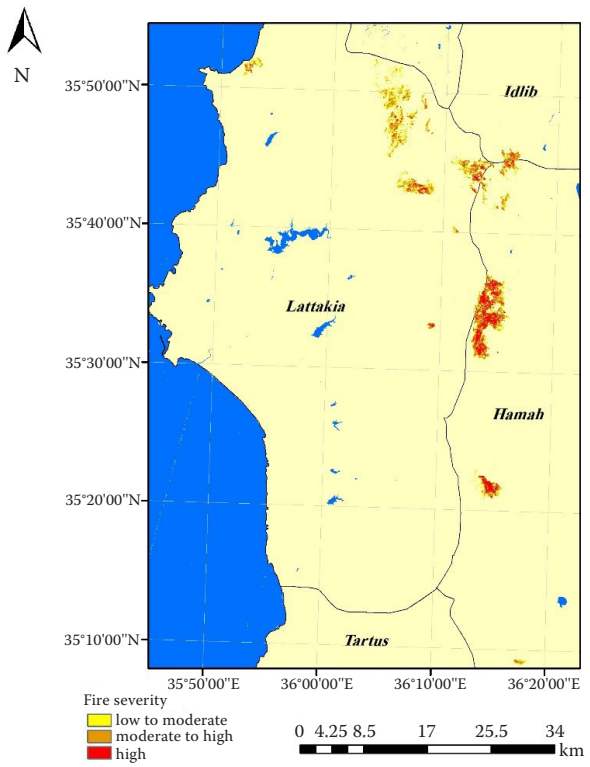

Figure 2. The Differenced Normalized Burn Ration (*dNBR*) map (September 27th, 2020)

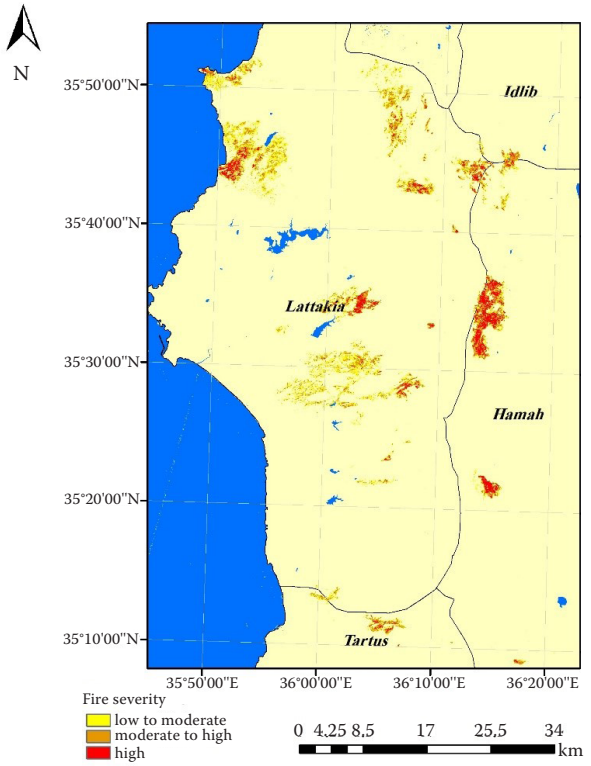

Figure 3. The Differenced Normalized Burn Ration (*dNBR*) map (October 22nd, 2020)

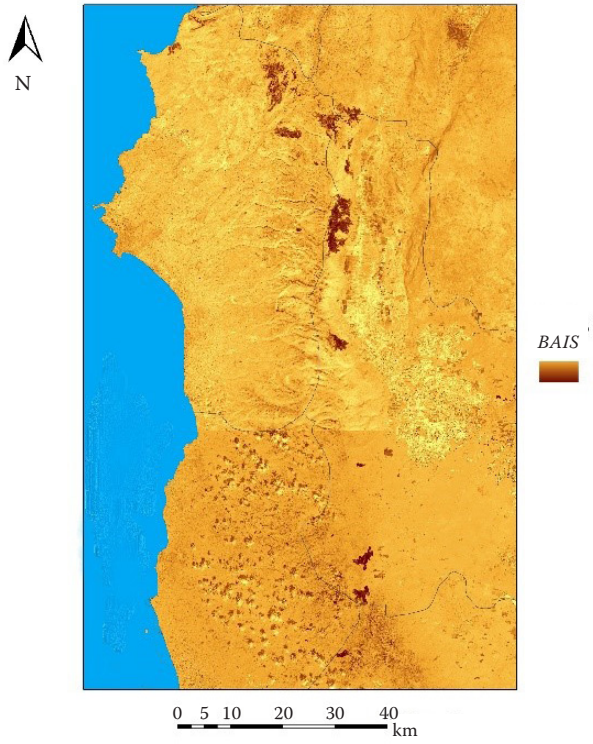

Figure 4. The post-fire Difference Burned Area Index for Sentinel-2 (*dBAIS2*) map (September 27th, 2020)

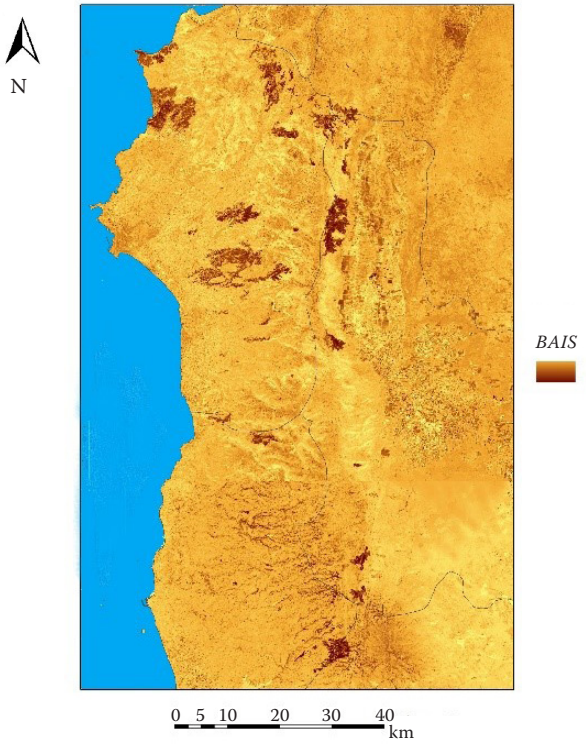

Figure 5. The post-fire Difference Burned Area Index for Sentinel-2 (*dBAIS2*) map (October 22nd, 2020)

https://doi.org/10.17221/122/2021-JFS

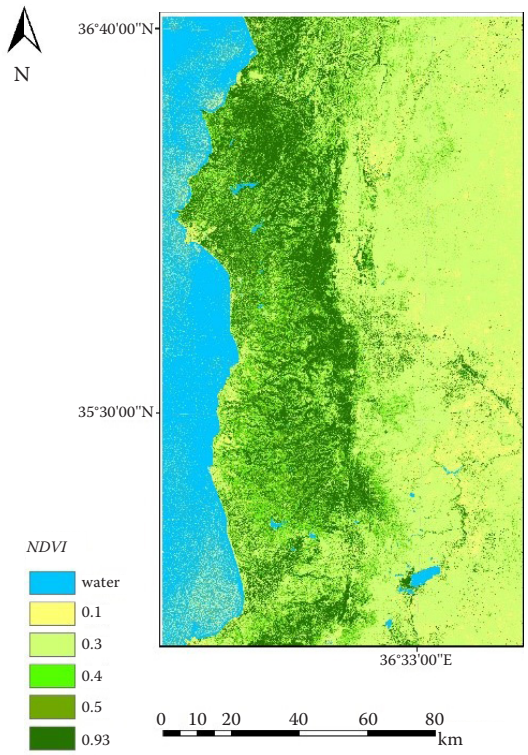

Figure 6. The pre-fire Normalized Difference Vegetation Index (*NDVI*) map (before the fire)

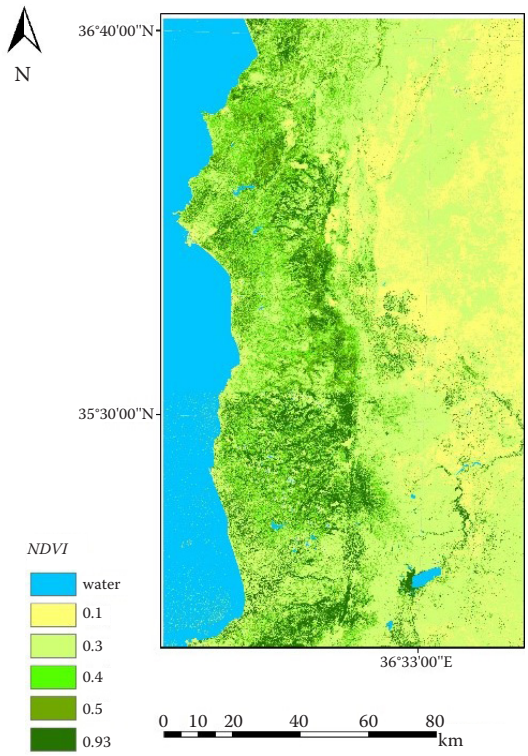

Figure 7. The post-fire Normalized Difference Vegetation Index (*NDVI*) map (September 27th, 2020)

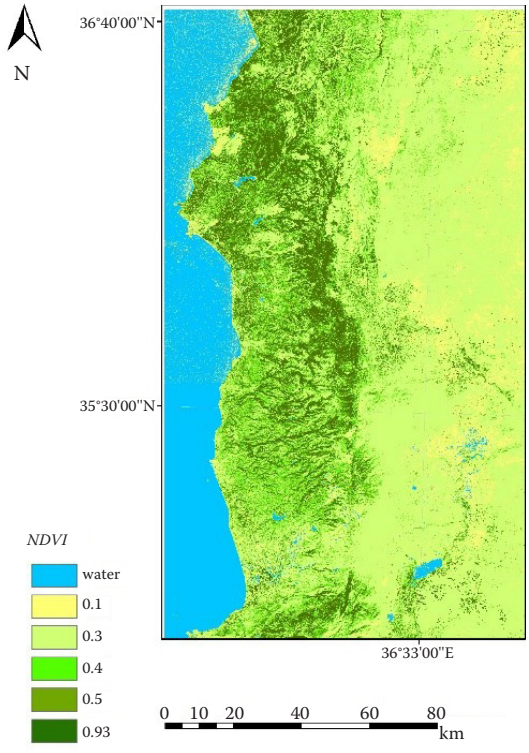

Figure 8. The post-fire Normalized Difference Vegetation Index (*NDVI*) map (October 22nd, 2020)

index (Difference Burned Area Index for Sentinel-2) is calculated from the arithmetic difference between the pre-fire *BAIS*2 values and the post-fire *BAIS*2 values, and the difference indices (such as *dBAIS*2 and *dNBR*) have been shown to have better results compared to the results with the *NBR* and *dNBR* indices (Sommai 2020). Figures 4 and 5 illustrate *dBAIS*2 index in the burned area.

In addition, *NDVI* was calculated using images taken just before and after the burning to determine the status of the vegetation before and after the occurrence of fire (Figures 6–8). The *NDVI* indicator has also been calculated for the burned area outlined in the study area. It is understood that the number of dense vegetation and moderate vegetation classes decreased, while the pixels in the sparse vegetation class increased according to *NDVI* (Table 4).

Moreover, in the *NDVI* maps obtained after the fire, the pixel values ranged between 0.1 and 0.3 for the destroyed area by the fire. Therefore, these areas were classified as sparse vegetation and moderate vegetation (Rutkay et al. 2020) (Figure 9).

Accuracy assessment. For evaluating the accuracy of *dNBR*, *BAIS*2 and *NDVI*, spectral indi-

https://doi.org/10.17221/122/2021-JFS

Table 4. Vegetation density level pre- and post-fire

Vegetation density	Pre-fire	Post-fire (September 27th, 2020)	Post-fire (October 22nd, 2020)
		(m^2)	
Low	4 165 006.08	3 836 366.92	1 182 436.68
Moderate	617 231.56	636 897.36	145 178.96
High	1 469 461.04	710 619.92	241 967.80

Table 5. Soil textural classes and variation in soil fertility before and after the fire at three places for different depths

Site	Fire status	Depth (cm)	Sand (%)	Silt (%)	Clay (%)	*EC* (Siemens·m^{-1})	pH	OM (%)
1	burned	0–10	49.5	26.0	24.5	0.577	7.935	4.844
		10–20	47.6	25.2	27.2	0.571	7.853	4.321
		20–30	49.5	24.0	26.5	0.580	7.957	4.547
	unburned	0–10	41.0	28.5	30.5	0.572	7.911	5.807
		10–20	42.0	30.2	27.8	0.532	7.041	4.415
		20–30	39.5	30.0	30.5	0.544	7.902	3.975
2	burned	0–10	49.5	21.0	26.5	0.635	7.941	5.561
		10–20	45.0	24.7	28.3	0.642	7.922	4.899
		20–30	48.5	22.5	27.5	0.691	7.868	4.925
	unburned	0–10	45.5	28.0	29.5	0.517	7.868	6.772
		10–20	46.0	25.0	30.0	0.535	7.698	6.110
		20–30	44.0	28.5	29.0	0.597	7.854	5.561
3	burned	0–10	45.3	25.0	26.2	0.707	7.352	3.542
		10–20	44.2	27.2	26.6	0.699	7.423	3.021
		20–30	44.7	29.0	25.0	0.692	7.032	2.959
	unburned	0–10	40.8	33.0	29.7	0.675	7.151	6.117
		10–20	42.1	30.6	27.3	0.601	7.011	5.632
		20–30	43.0	32.0	26.3	0.558	6.607	4.905

EC – electrical conductivity; OM – organic matter

ces were derived from Sentinel satellite imagery in identifying burned areas. 132 random points were used to calculate the overall accuracy, which is the ratio of the number of correctly classified samples to the total number of samples (Congalton et al. 1983). The overall accuracy was 87.4% of the *DNBR* index, 90.2% of the *BAIS*2 index, and 82.4% of the *NDVI* index, which corresponds with a high classification precision (Fleiss et al. 2013).

The effect of fire on the availability of soil nutrients. The results of this search indicated that the fire led to a change in some chemical properties of the soil during the burning process (Tables 5 and 6). The organic matter content in burned and unburned soils decreased significantly in the second and third location. However, there was no significant difference between the soil depths in the three locations. This result is due to burning organic matter during the fire thus reducing its soil content (Garcia-Marco, Gonzalez-Prieto 2008).

The pH values were significantly higher in the burned soil compared to the unburned soil only at the third site. Nevertheless, there was no significant difference in pH values between the depths of soils at the three studied sites. The difference between the burned and unburned soil can be due to the ash from combustion of the vegetation above the soil surface due to the fire, as part of this ash returns to the forest land and increases pH value due to its richness in soluble base cations and its

https://doi.org/10.17221/122/2021-JFS

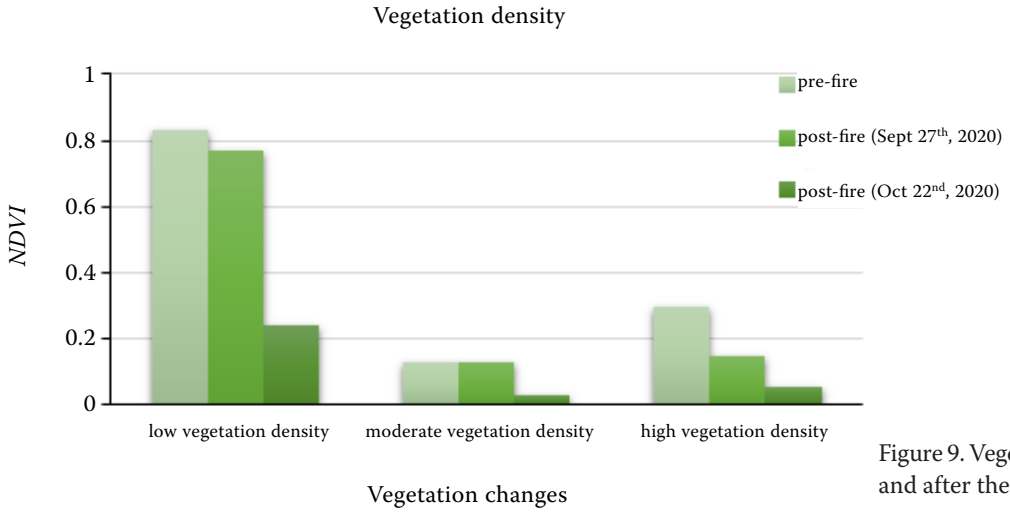

Figure 9. Vegetation changing before and after the fire

infiltration with water into the soil after rain. This is consistent with findings of Ershad et al. (2013). The EC values of the burned soil were higher compared to the unburned soil. It was significantly different at the second site, and significantly different at the third soil depth compared to unburned soils. This is due to a release of mineral ions from deposited ash and combusted organic matter (Hernandez et al. 1997; Certini 2005). An increase in sand percentage at the three sites was significant at the first and second depth at the first site, with a decrease in the percentage of silt at the three sites, and it was significant at the first site. As for the clay, its percentage was decreased at the three sites, but

Table 6. Variation in soil fertility before and after the fire at three places for different depths

Site	Fire status	Depth (cm)	N	P	K	Fe	Mn	Cu	Zn
						(ppm)			
1	burned	0–10	0.294	5.430	130.6	2.456	1.670	1.602	1.100
		10–20	0.225	5.065	175.9	2.012	1.665	1.610	0.986
		20–30	0.224	4.178	224.6	2.267	1.642	1.038	0.847
	unburned	0–10	0.258	0.994	105.0	1.828	1.703	1.544	1.038
		10–20	0.202	1.302	87.9	1.903	1.801	1.453	0.973
		20–30	0.196	1.518	79.9	2.142	1.675	1.100	0.773
2	burned	0–10	0.308	5.195	533.9	3.030	1.646	2.647	0.636
		10–20	0.332	5.032	412.4	3.065	1.602	2.499	0.676
		20–30	0.418	4.367	330.9	3.093	1.640	2.643	0.416
	unburned	0–10	0.292	4.418	330.4	2.922	1.607	2.497	0.633
		10–20	0.281	3.892	255.3	2.865	1.544	2.423	0.471
		20–30	0.262	3.492	236.3	3.063	1.573	2.199	0.410
3	burned	0–10	0.442	5.012	499.9	3.334	2.111	1.939	0.711
		10–20	0.401	5.601	445.0	3.712	2.030	2.034	0.687
		20–30	0.399	4.980	449.4	3.233	2.301	2.026	0.602
	unburned	0–10	0.376	4.993	301.8	2.055	2.010	1.655	0.544
		10–20	0.383	4.235	305.7	2.224	1.879	1.436	0.505
		20–30	0.399	3.639	311.4	2.237	1.901	1.518	0.498

https://doi.org/10.17221/122/2021-JFS

the decrease was significant only at the second site. Nevertheless, there was no significant difference in the depths of soil at the three sites.

Moreover, the fire led to an increase in the solubility of the available major soil elements N, P and K. This is due to the ash with a high content of carbonates and oxides, which precipitated on the surface layer of soil (Capulin-Grande et al. 2018), for N this increase was significant at the first site, and it was significant at the second and third depth.

The results showed that the pre- and post-fire available phosphorus concentration in soils was significantly different at the first and second site. However, this difference was significant at the second depth at the second site only. It was found that the pre- and post-fire concentration of potassium available in soils was significant at the first and second site, but this difference was not significant at particular depths of soil between burned and unburned soil.

An increase was revealed in the solubility of the soil microelements Zn, Cu, Mn and Fe. This increase was significant at the third site for Fe. However, no significant difference was observed between the burned and unburned soils at particular depths. The second site was found to have the maximum concentration of Mn compared to the other sites. In addition, the fire had no significant effect on the depths of the soil.

Moreover, fires led to a significant decrease in Cu and Zn at the third site but this change in the Zn and Cu concentrations was not significant between burned and unburned soils at particular soil depths.

CONCLUSION

The findings of the study can help the forest management measures planning required to retrieve forest cover effectively. It is thought that using higher resolution satellite Sentinel-2A images will increase the accuracy of the study. When the change detection analysis in Sentinel-2A images and *NBR*, *dNBR*, *BAIS*2 and *NDVI* indices were used, it was possible to identify the burned area in the study area and risk classes for future fires in this region were estimated, besides the detection of vegetation that was destroyed by fire was also carried out. In addition, as a consequence, the map of this region was created with elevated accuracy.

The results of this study indicated that combustion had a significant effect on dissolved cations in the soil. In contrast, the increased availability of soil nutrients after a fire is caused by forest ash deposits and the products of soil organic matter oxidation resulting from the fire. In general, in all instances, there was a trend towards a high gear of soil nutrients in the burned soils.

REFERENCES

Ali M. (2000): An analytical study of forest fires in Lattakia and Lug (Syria). Tishreen University Magazine for Studies and Research – Agricultural Science Series, 26: 213–224. (in Arabic)

Ali M. (2004): Science of Forest Soil. Latakia, Tishreen University Publications, Faculty of Agriculture: 337. (in Arabic)

Bassi S., Kettunen M. (2008): Forest Fires: Causes and Contributing Factors in Europe. London, European Parliament's Committee on the Environment, Public Health and Food Safety: 56.

Boer M., Macfarlane C., Norris J., Sadler R.J., Wallece J., Grierson P.F. (2008): Mapping burned areas and burn severity patterns in SW Australian eucalypt forest using remotely-sensed changes in leaf area index. Remote Sensing of Environment, 112: 4358–4369.

Bremner M. (1996): Nitrogen total. In: Sparks D.L. (ed.): Methods of Soil Analysis Part 3: Chemical Methods. Madison, Soil Science Society of America: 1085–1121.

Brewer C.K., Winne J.C., Redmond R.L., Opitz D.W., Mangrich M.V. (2005): Classifying and mapping wildfire severity: A comparison of methods. Photogrammetric Engineering and Remote Sensing, 71: 1311 –1320.

Canbaz O., Gürsoy Ö., Gökçe A. (2018): Detecting clay minerals in hydrothermal alteration areas with integration of ASTER image and spectral data in Kösedag-Zara (Sivas), Turkey. Journal of the Geological Society of India, 91: 483–488.

Capulin-Grande J., Islas A.S., Rodríguez-Laguna R., Sánchez J.J.M., Zárate R.R., Islas-Santillán M. (2018): Influence of fire on soil and vegetation properties in two contrasting forest sites in Central México. Ciencia e investigación agraria: Revista latinoamericana de ciencias de la agricultura, 45: 128–137.

Certini G. (2005): Effects of fire on properties of forest soils: A review. Oecologia, 143: 1–10

Chen X., Vogelmann J.E., Rollins M., Ohlen D., Key C.H., Yang L., Huang C., Shi H. (2011): Detecting post-fire burn severity and vegetation recovery using multitemporal remote sensing spectral indices and field-collected composite burn index data in a ponderosa pine forest. International Journal of Remote Sensing, 32: 7905–7927.

Congalton R.G., Green K. (2019): Assessing the Accuracy of Remotely Sensed Data: Principles and Practices. Boca Raton, CRC Press: 328.

https://doi.org/10.17221/122/2021-JFS

Congalton R., Mead R. (1983): A quantitative method to test for consistency and correctness in photointerpretation. Photogrammetric Engineering and Remote Sensing, 49: 69–74.

Conyers M., Davey B. (1988): Observations on some routine methods for soil pH determination. Soil Science, 145: 29–36.

Davies T.M. (2016): The Book of R: A First Course in Programming and Statistics. San Francisco, No Starch Press: 835.

Elvidge C.D. (1990): Visible and near infrared reflectance characteristics of dry plant materials. International Journal of Remote Sensing, 11: 1775–1795.

Ershad M., Hemmati V., Hashemi S.A., Foroozan A.H. (2013). The effect of fires on the chemical properties of soil in Nortern Iran: A case study on *Pinus taeda* stands. Bulletin of Environment, Pharmacology and Life Sciences, 2: 51–54.

Espelta J.M., Verkaik I., Eugenio M., Lloret F. (2008): Recurrent wildfires constrain long-term reproduction ability in *Pinus halepensis* Mill. International Journal of Wildland Fire, 17: 579–585.

FAO (2005): Integrated forest fire management project in a participatory approach in Syria.GCP /SYR /010/ITA: 83.

Fernández-Manso A., Quintano C. (2015): Evaluating Landsat ETM+ emissivity-enhanced spectral indices for burn severity discrimination in Mediterranean forest ecosystems. Remote Sensing Letters, 6: 302–310.

Fleiss J.L., Levin B., Paik M.C. (2013). Statistical Methods for Rates and Proportions. Somerset, John Wiley & Sons: 723.

Forestry and Reforestations Directorate (2005): Integrated management strategy for forest fires participatory approach in Syria. Ministry of Agriculture and Agrarian Reform and FAO, Integrated Forest Fire Management Participation Project.GCP/SYR/010/ITA: 83.

Francos M., Úbeda X., Tort J., Panereda J.M., Cerda A. (2016): The role of forest fire severity on vegetation recovery after 18 years. Implications for forest management of *Quercus suber* L. in Iberian Peninsula. Global and Planetary Change, 145: 11–16.

Gee W., Or D. (2002): Particle-size analysis. In: Dane J.H., Topp G.C. (eds): Methods of Soil Analysis Part 4: Physical Methods. Madison, Soil Science Society of America: 255–293.

Gupta S., Roy A., Bhavsar D., Kala R., Singh S., Kumar A.S. (2018): Forest fire burnt area assessment in the biodiversity rich regions using geospatial technology: Uttarakhand forest fire event 2016. Journal of the Indian Society of Remote Sensing, 46: 945–955.

Hernández T., Garcia C., Reinhardt I. (1997): Short-term effect of wildfire on the chemical, biochemical and microbiological properties of Mediterranean pine forest soils. Biology and Fertility of Soils, 25: 109–116.

Kalkan K., Maktav M.D. (2018): A cloud removal algorithm to generate cloud and cloud shadow free images using information cloning. Journal of the Indian Society of Remote Sensing, 46: 1255–1264.

Kasas H. (2008): The study of natural renewal for the cultural cane, *Pinus brutia.* Ten for the fire of the simple 2004 and its social and economic dimensions. [MSc. Thesis.] Latakia, University of Tishreen. (in Arabic)

Kerr J.T., Ostrovsky M. (2003): From space to species: Ecological applications for remote sensing. Trends in Ecology and Evolution, 18: 299–305.

Key C.H., Benson N.C. (2006): Landscape assessment: Ground measure of severity, the Composite Burn Index; and remote sensing of severity, the Normalized Burn Ratio. In: Lutes D.C., Keane R.E., Caratti J.F., Key C.H., Benson N.C., Sutherland S., Gangi L.J. (eds): FIREMON: Fire Effects Monitoring and Inventory System. Fort Collins, U.S. Department of Agriculture, Forest Service, Rocky Mountains Research Station: 55.

Kuo S. (1996): Phosphorus. In: Sparks D.L. (ed.): Methods of Soil Analysis Part 3: Chemical Methods. Madison, Soil Science Society of America: 869–920.

Loeppert H., Inskeep P. (1996): Iron. In: Sparks D.L. (ed.): Methods of Soil Analysis Part 3: Chemical Methods. Madison, Soil Science Society of America: 639–664.

Main-Knorn M., Pflug B., Louis J., Debaecker V., Müller-Wilm U., Gascon F. (2017): Sen2Cor for Sentinel-2. Image and Signal Processing for Remote Sensing XXIII, 10427: 1042704.

Matin M.A., Chitale V.S., Murthy M.S., Uddin K., Bajracharya B., Pradhan S. (2017): Understanding forest fire patterns and risk in Nepal using remote sensing, geographic information system and historical fire data. International Journal of Wildland Fire, 26: 276–286.

Navarro G., Caballero I., Silva G., Parra P.C., Vázquez A., Calderia R. (2017): Evaluation of forest fire on Madeira Island using Sentinel-2A MSI imagery. International Journal of Applied Earth Observation and Geoinformation, 58: 97–106.

Nelson W., Sommers E. (1996): Total carbone, organic carbone, and organic matter. In: Sparks D.L. (ed.): Methods of Soil Analysis Part 3: Chemical Methods. Madison, Soil Science Society of America: 961–1010.

Pausas J.G. (2004): Changes in fire and climate in the eastern Iberian Peninsula (Mediterranean basin). Climatic Change, 63: 337–350.

Pausas J.G., Llovet J., Rodrigo A., Vallejo R. (2008): Are wildfires a disaster in the Mediterranean basin? A review. International Journal of Wildland Fire, 17: 713–723.

Quintano C., Fernández-Manso A., Fernández-Manso O. (2018): Combination of Landsat and Sentinel-2 MSI data for initial assessing of burn severity. International Journal of Applied Earth Observation and Geoinformation, 64: 221–225.

Rhoades D. (1996): Salinity: Electrical conductivity and total dissolved solids. In: Sparks D.L. (ed.): Methods of Soil

https://doi.org/10.17221/122/2021-JFS

Analysis Part 3: Chemical Methods. Madison, Soil Science Society of America: 417–435.

Roteta E., Bastarrika A., Padilla M., Storm T., Chuvieco E. (2019): Development of a Sentinel-2 burned area algorithm: Generation of a small fire database for sub-Saharan Africa. Remote Sensing of Environment, 222: 1–17.

Rowell A., Moore F. (2002): Global Review of Forest Fires. Gland, Forests for Life Programme Unit, WWF International: 64.

Rutkay A., Kalkan K., Gürsoy Ö. (2020): Determining the forest fire risk with Sentinel 2 images. Turkish Journal of Geosciences, 1: 22–26.

Santana N.C., de Carvalho Júnior O.A., Gomes R.A.T., Guimarães R.F. (2018): Burned-area detection in Amazonian environments using standardized time series per pixel in MODIS data. Remote Sensing, 10: 1904.

SCBD (Secretariat of the Convention on Biological Diversity) (2001): Impacts of Human-Caused Fires on Biodiversity and Ecosystem Functioning, and Their Causes in Tropical, Temperate and Boreal Forest Biomes. Montreal, SCBD: 38.

Sommai C. (2020): Forest fire damage assessment and biomass loss using Sentinel-2 satellite imagery in Doi Inthanon National Park in Chiangmai Province, Thailand. [MSc. Thesis.] Saen Suk, Burapha University.

Suarez L. (1996): Berylium, magnesium, calcium, strontium, and barium. In: Sparks D.L. (ed.): Methods of Soil Analysis Part 3: Chemical Methods. Madison, Soil Science Society of America: 575–601.

Sugihara N.G., Van Wagtendonk J.W., Fites-Kaufmann J., Shaffer K.E., Thode A.E. (2006): Fire in California Ecosystems. Berkeley, University of California Press: 596.

Ursino N., Rulli C. (2010): Combined effect of fire and water scarcity on vegetation patterns in arid lands. Ecological Modelling, 221: 2353–2362.

Veraverbeke S., Lhermitte S., Verstraeten W.W., Goossens R. (2011): A time-integrated MODIS burn severity assessment using the multi-temporal differenced normalized burn ratio (*dNBR*MT). International Journal of Applied Earth Observation and Geoinformation, 13: 52–58.

Yurtseven H. (2014): Using of high resolution satellite images in object based image analysis. [Ph.D. Thesis.] Istanbul, Istanbul University, Graduate School of Science and Engineering.

Yuan C., Liu Z., Zhang Y. (2017): Aerial images-based forest fire detection for firefighting using optical remote sensing techniques and unmanned aerial vehicles. The Journal of Intelligent and Robotic Systems, 88: 635–654.

Received: October 2, 2021
Accepted: February 22, 2022